

# involve

a journal of mathematics

## Perimeter-minimizing pentagonal tilings

Ping Ngai Chung, Miguel A. Fernandez,  
Niralee Shah, Luis Sordo Vieira and Elena Wikner





# Perimeter-minimizing pentagonal tilings

Ping Ngai Chung, Miguel A. Fernandez,  
Niralee Shah, Luis Sordo Vieira and Elena Wikner

(Communicated by Michael Dorff)

We provide examples of perimeter-minimizing tilings of the plane by convex pentagons and examples of perimeter-minimizing tilings of certain small flat tori.

## 1. Introduction

**Cairo-prismatic tilings.** Thomas C. Hales [2001] proved the *honeycomb conjecture*, which says that regular hexagons provide a least-perimeter unit-area way to tile the plane. Squares and equilateral triangles, though less efficient than hexagons, provide a least-perimeter unit-area tiling by quadrilaterals and triangles.

It is interesting to ask about a least-perimeter unit-area *pentagonal* tiling, because regular pentagons do not tile the plane. Chung et al. [2012, Theorem 3.5] proved that among all convex unit-area pentagonal tilings of the plane and of appropriate flat tori, there are two that minimize perimeter: the *Cairo* and *prismatic* pentagons, defined as the unit-area pentagons having only  $90^\circ$  and  $120^\circ$  angles and circumscribed to a circle. The prismatic pentagon has adjacent right angles, and its sides (starting from the vertex along the axis of symmetry) are in the ratio  $1 : \frac{1}{2}(\sqrt{3}+1) : \sqrt{3}$ , while the Cairo pentagon has nonadjacent right angles, and its sides are in the ratio  $1 : 1 : \sqrt{3}-1$ . See Figure 1.

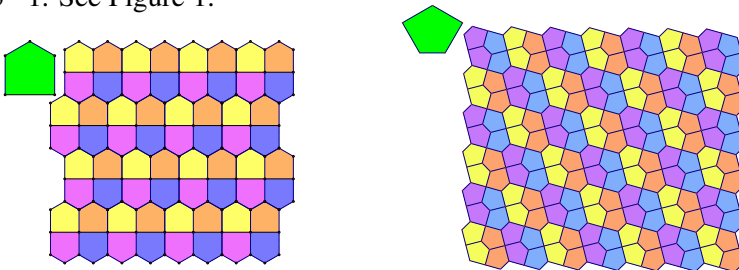


**Figure 1.** In green, the prismatic pentagon (left) and the Cairo pentagon (right). Each is a minimum-perimeter pentagonal tiler.

*MSC2010:* primary 52C20; secondary 52C05.

*Keywords:* tilings, pentagon, isoperimetric.

Building on this, we show in Propositions 2.3 and 2.4 below that each of these two polygons admits a unique monohedral edge-to-edge tiling. We also discuss mixed Cairo-prismatic tilings. Such tilings have been known at least since Marjorie Rice discovered a nonperiodic,  $D_6$ -symmetry example, first published as Figure 15 in [Schattschneider 1981] and shown also in [Chung et al. 2012], together with a number of other examples we have found (see Figures 11–23 below for a sampling).

**Restrictions on nonconvex tilings.** Can one beat the Cairo and prismatic pentagons by allowing nonconvex pentagonal shapes? In [Chung et al. 2012] (remark after Theorem 3.5) we conjectured that the answer is negative. Here we make some progress toward a proof: Proposition 2.10 below states that any tiling by unit-area nonconvex pentagons must have perimeter greater than a Cairo or prismatic tiling. Proposition 2.11 states that if a mixture of unit-area convex and nonconvex pentagons is perimeter-minimizing, then the ratio of the numbers of convex to nonconvex pentagons must be greater than 2.6. This provides a tool to investigate the problem further in Section 3.

**Minimal tilings on flat tori.** Section 3 considers minimal tilings of small flat tori, which correspond to doubly periodic planar tilings. Proposition 3.3 states that the unique perimeter-minimizing edge-to-edge pentagonal tiling of a certain flat torus of area 2 is by prismatic pentagons, as shown in Figure 26. Similarly, Proposition 3.9 states that the unique perimeter-minimizing pentagonal tiling of the square torus of area 4 is by Cairo pentagons, as shown in Figure 2. Both these results allow for mixtures of nonconvex and convex pentagons.

The proofs depend on two main lemmas: Lemma 3.5 places a lower bound on the perimeter of a unit-area convex pentagon with a given small angle  $\alpha$ , and Lemma 3.8 places a lower bound on the perimeter of a nonconvex pentagon given two edges and the included angle.

We follow Proposition 3.9 by considering minimal tilings on other small flat tori and flat Klein bottles. Conjecture 3.4 proposes the minimal pentagonal tiling of the square torus of area 2. Conjecture 3.12 proposes minimal polygonal tilings for the square tori of areas 2, 3 and 4. Proposition 3.13 provides a lower bound on the perimeters of tilings of flat Klein bottles, and provides perimeter-minimizing tilings of many flat Klein bottles, as in Figure 35, right.

## 2. Cairo-prismatic tilings

**Definition 2.1.** A *tiling* is a decomposition of a surface into a union of simply connected disjoint open sets and their boundaries. The closure of each open set is called a *tile*. This paper focuses on tilings by unit-area pentagons. The Cairo and prismatic pentagons were defined on page 453; both have perimeter  $\sqrt{2}(1 + \sqrt{3}) \approx 3.86$ . We define the *perimeter ratio* of a tiling of the plane to be the limit superior as

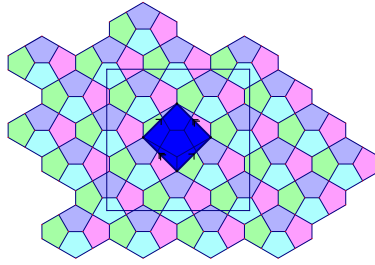


**Figure 2.** Cairo tiling on square torus of area 4.

$r$  approaches infinity of the perimeter of the tiling inside a disc of radius  $r$  centered at the origin divided by  $\pi r^2$ . A *monohedral tiling* is a tiling by a single prototile.

**Proposition 2.2** [Chung et al. 2012, Theorem 3.5]. *Perimeter-minimizing tilings of the plane by unit-area convex polygons with at most five sides are given by Cairo and prismatic tiles, as in Figure 1.*

**Remark.** Chung et al. remark that every doubly periodic perimeter-minimizing tiling by convex pentagons consists of Cairo and prismatic tiles. Of course, if allowed to break symmetry, one can alter a compact region arbitrarily without changing the limiting perimeter ratio.

Next we state and prove Propositions 2.3 and 2.4.

**Proposition 2.3.** *The Cairo pentagonal tiling shown in Figure 1, right, is the unique tiling by Cairo pentagons.*

*Proof.* Consider a single Cairo prototile  $C_0$  with one side of length  $a$  and four sides of length  $b$ . The side of length  $a$  determines the orientation of the adjacent Cairo tile  $C_1$ , as shown in Figure 3. Furthermore, in a Cairo tile there is only one  $120^\circ$  angle with adjacent sides both of length  $b$ , which determines the orientations of tiles  $C_2$  and  $C_3$ . Thus, as shown in Figure 3, each Cairo tile must be in a hexagon with opposite edges of length  $a$  and the other four edges of equal length  $2b$ . We call this unit  $R_1$ . Using tiles  $C_2$  and  $C_3$ ,  $R_1$  determines vertical hexagons to its left and right. Similarly, these vertical hexagons each determine two horizontal hexagons above and below themselves. Therefore,  $R_1$  determines horizontal hexagons to its upper and lower left and right. Similarly, each of those horizontal hexagons determine four adjacent horizontal hexagons (among which are the other two hexagonal neighbors of  $R_1$ ). Continuing in this manner, a complete tiling by these horizontal hexagons is determined, and therefore the unique tiling, up to isometry, by Cairo pentagons is the tiling shown in Figure 1, right.  $\square$

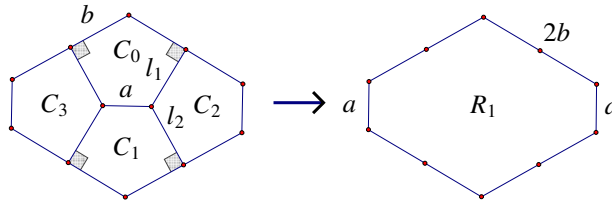


**Figure 3.** A Cairo tiling must be a tiling by hexagons with opposite edges of length  $a$  and the other four edges of equal length  $2b$  ( $R_1$ ).

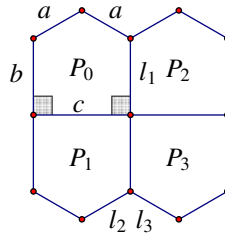


**Figure 4.** A prismatic pentagonal tiling must be a tiling by the hexagon with opposite edges of length  $2b$  and the other four edges of equal length  $a$ .

Notice that if we do not require edge-to-edge, then the prismatic tiling is not unique, as shown in Figure 10. On the other hand, if edge-to-edge is required, then the edge between the right angles has the unique length and determines the tiling:

**Proposition 2.4.** *The prismatic tiling as shown in Figure 1, left, is the unique edge-to-edge tiling by prismatic pentagons.*

*Proof.* Consider a single prismatic prototile  $P_0$ . The unique edge of length  $c$  determines the orientation of the adjacent prismatic tile  $P_1$ . Thus, a prismatic pentagonal tiling must be a tiling by the hexagon with opposite edges of length  $2b$  and the other four edges of equal length  $a$ , as shown in Figure 4. Furthermore, the length  $b$  of edge  $l_1$  and the adjacent  $90^\circ$  angle determine the orientation of the adjacent prismatic tile  $P_2$ , which in turn determines the orientation of  $P_3$ . Continuing in this way, we construct a row of hexagons, each consisting of two prismatic pentagons, as shown in Figure 4. Note that the edges of length  $l_2$  and  $l_3$  determine the orientation of  $P_4$ . By a similar argument to that for  $P_0$ , the edge of length  $c$  of the tile  $P_4$  determines the orientation of the adjacent prismatic tile, establishing another row of two-prismatic hexagons, as shown in Figure 5. Continuing in this manner, we find that the unique edge-to-edge tiling by prismatic pentagons is, up to isometry, the prismatic tiling defined in Figure 1, right.  $\square$

For a monohedral tiling, denote the ordered degrees  $v_1, v_2, \dots, v_n$  of the vertices of a tile by  $[v_1, v_2, \dots, v_n]$ . Given the characterization of perimeter-minimizing

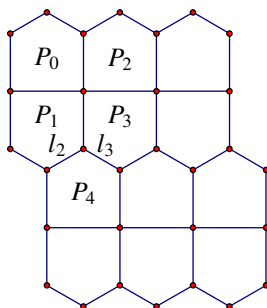


**Figure 5.** The edges of length  $l_2$  and  $l_3$  determine the orientation of  $P_4$ , which determines another row of two-prismatic hexagons.

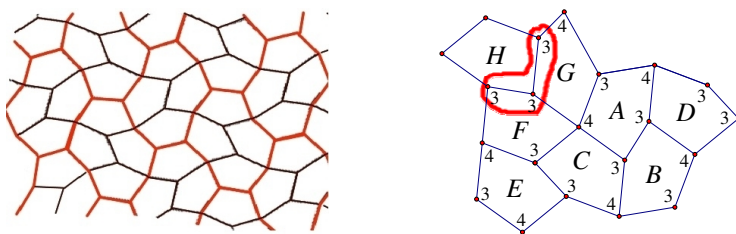


**Figure 6.** Left: the unique monohedral tiling with vertex degrees  $[3, 3, 4, 3, 4]$  (picture is taken from an earlier version of [Li et al. 2011]). Right: illustration of a contradiction in the proof of Proposition 2.5.

tilings by convex pentagons by Chung et al. [2012, Theorem 3.5], it is natural to ask whether the Cairo and prismatic tilings are the only monohedral tilings with the vertex degrees  $[3, 3, 4, 3, 4]$  and  $[3, 3, 3, 4, 4]$ , respectively.

Proposition 2.5 shows that any monohedral tiling with vertex degrees  $[3, 3, 4, 3, 4]$  is combinatorially equivalent to the tiling in Figure 6, left. Indeed, there are only two such tilings up to linear equivalence. Proposition 2.6 shows uncountably many distinct edge-to-edge tilings with vertex degrees  $[3, 3, 3, 4, 4]$  that are not equivalent under a linear map.

**Proposition 2.5.** *The tiling in Figure 6, left, is the unique tiling, up to combinatorial equivalence, by congruent tiles with vertex degrees  $[3, 3, 4, 3, 4]$ .*

*Proof.* Consider a single prototile  $A$  with vertex degrees  $[3, 3, 4, 3, 4]$  as shown in Figure 7. Then the edge connecting the vertices of degree 3 determines the degrees of the other three vertices of the adjacent tile  $B$ . Furthermore, each vertex of degree 3 shared by tiles  $A$  and  $B$ , as well as the two vertices of degree 4 adjacent to them, determine the degrees of the remaining two vertices of tiles  $C$  and  $D$ . Now, given the edge of  $C$  connecting the vertices of degree 3, the remaining three vertices

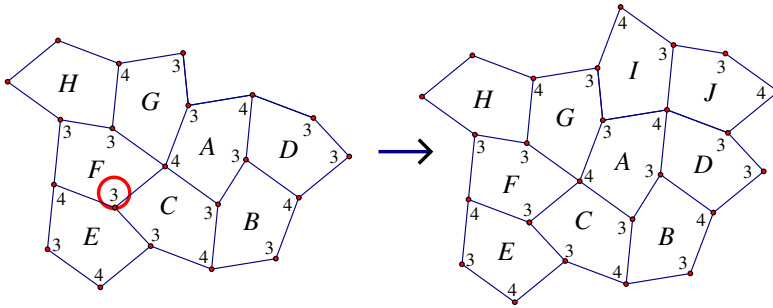


**Figure 7.** Unique monohedral tiling with vertex degrees  $[3, 3, 4, 3, 4]$  up to combinatorial equivalence.

of the tile  $E$  are determined. The vertex of degree 3 circled in red and the adjacent vertices of degree 4 determine the degrees of the remaining two vertices of  $F$ . Now consider the tile  $G$ , which has three vertices determined by the adjacent tiles  $A$  and  $F$ . Suppose the vertex adjacent to the vertex of degree 3 shared with  $F$  was degree 3. Then the tile  $H$  adjacent to  $F$  and  $G$  would have three adjacent vertices of degree 3, a contradiction (Figure 6, right). Thus, this vertex in  $G$  must be of degree 4 and the remaining vertex is of degree 3. By a parallel argument, the vertex degrees of tile  $I$  are determined. Thus, the degrees of the vertices of all the tiles adjacent to  $A$  are determined. Continuing in this way, we can construct the tiling show in Figure 6, left. It follows that this is the unique tiling up to combinatorial equivalence by congruent tiles with vertex degrees  $[3, 3, 4, 3, 4]$ .  $\square$

**Proposition 2.6.** *Given vertex degrees  $[3, 3, 3, 4, 4]$ , there are uncountably many monohedral edge-to-edge tilings that are not equivalent under a linear mapping.*

*Proof.* Take the prismatic tile and deform the line segments  $a$  and  $b$  of the pentagon as shown in Figure 8, left. Notice that each point on the line  $l$  has a different corresponding pentagon. There exists a monohedral tiling for each one of these prototiles with vertex degrees  $[3, 3, 3, 4, 4]$  (Figure 8, right). Therefore, there are

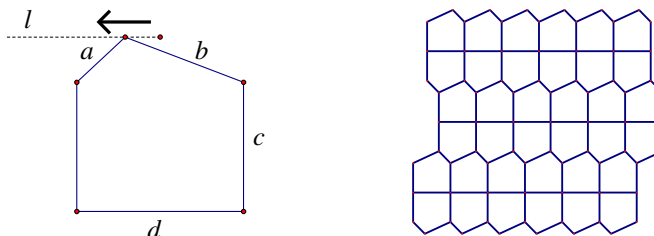


**Figure 8.** Left: different tiles with vertex degrees  $[3, 3, 3, 4, 4]$ . Right: a monohedral tiling with vertex degrees  $[3, 3, 3, 4, 4]$ .



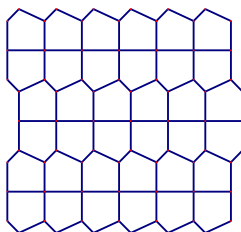


**Figure 9.** Another construction of a nonequivalent monohedral tiling with vertex degrees  $[3, 3, 3, 4, 4]$ .

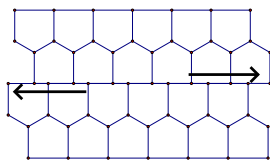


**Figure 10.** Prismatic tilings that are not edge-to-edge.

uncountably many monohedral, edge-to-edge tilings that are not equivalent under a linear mapping.  $\square$

**Remark.** Another construction of a nonequivalent monohedral tiling with vertex degrees  $[3, 3, 3, 4, 4]$  is as shown in Figure 9. Similarly, for the prismatic tiling, one can translate a row of prismatic tiles sideways as in Figure 10. There may be many more.

To further the results of [Chung et al. 2012] we found many examples of tilings by mixtures of Cairo and prismatic pentagons. These tilings now appear in [Chung et al. 2012]. Meanwhile we discovered a Cairo-prismatic tiling by Marjorie Rice [ $\geq 2014$ ; Schattschneider 1981, Figure 15] who constructed this tiling even before Chung et al. proved that the Cairo and prismatic tilings are perimeter-minimizing for convex pentagons. We classify these tilings by their wallpaper groups in Figures 11–17. Daniel Huson [ $\geq 2014$ ] has found tilings by many other pairs of prototiles.

**Definition 2.7** [Schattschneider 1978]. *Wallpaper groups* are groups of isometries which leave a tiling invariant under linear combinations of two linearly independent translation vectors. Note that any such tiling is doubly periodic and therefore tiles a flat torus.

For a chart of the 17 wallpaper groups and their respective symmetries, refer to [Schattschneider 1978] or [Wikipedia Commons 2011].

**Example 2.8.** Tilings of flat tori are sometimes categorized by their symmetries. Figures 11–17 are examples of Cairo and prismatic tilings for the listed wallpaper group.

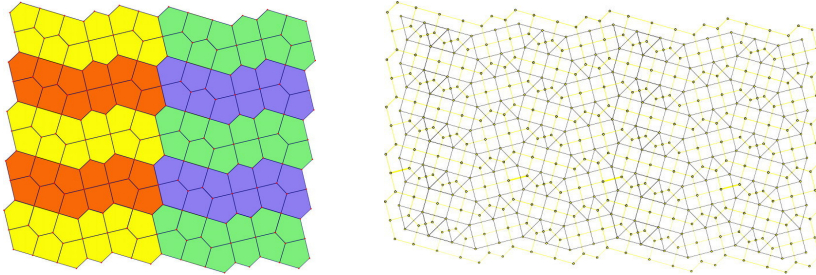


**Figure 11.** Tiling (left) and dual tiling (right) with  $p1$ .

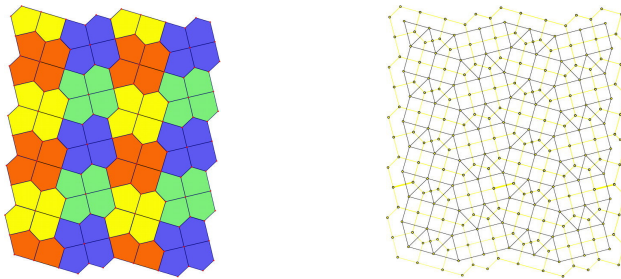


**Figure 12.** Tiling (left) and dual tiling (right) with  $p2$ .

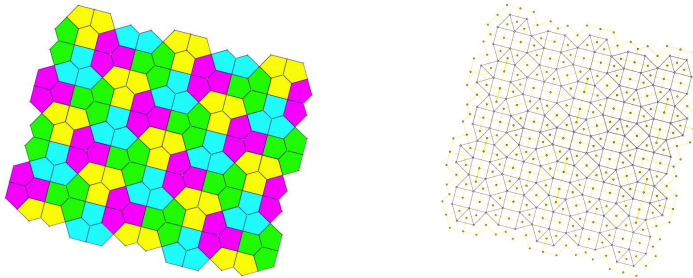


**Figure 13.** Tiling (left) and dual tiling (right) with  $p4g$ .

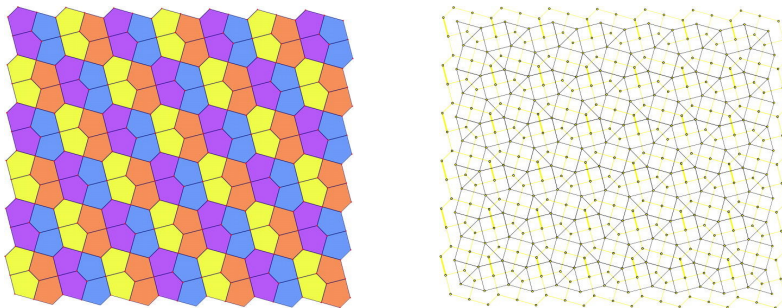


**Figure 14.** Cairo tiling with  $p4g$  (left) and its dual (right).

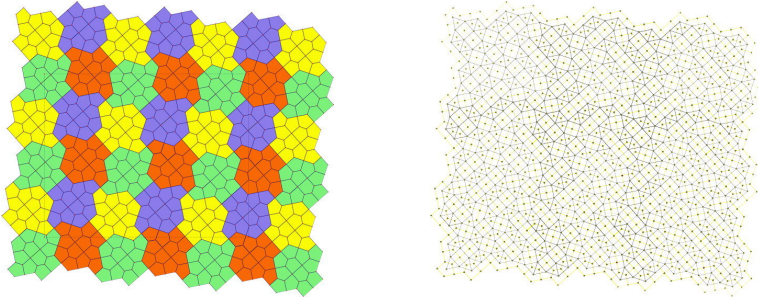


**Figure 15.** Spaceship tiling with  $p4g$  (left) and its dual (right).

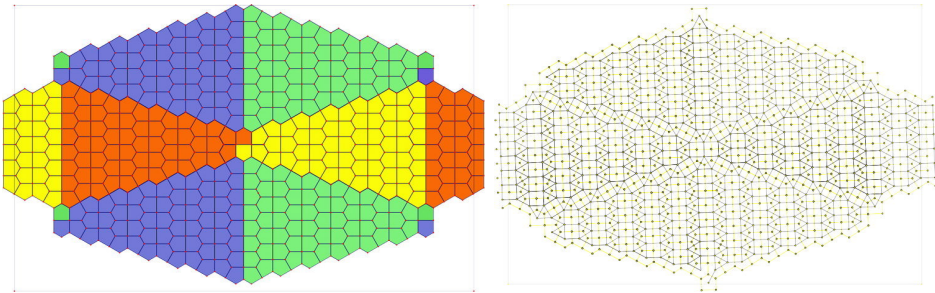


**Figure 16.** Christmas tree tiling with  $cmm$  (left) and its dual (right).

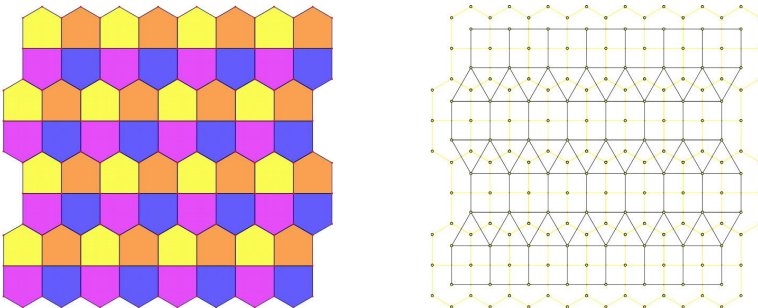


**Figure 17.** Prismatic tiling with  $cmm$  (left) and its dual (right).

**Remark.** We think Figure 12, left, gives the unique planar tiling with fundamental region consisting of only two Cairo tiles and two prismatic tiles, but we didn't need this fact.

**Example 2.9.** Figures 18–23 are examples of Cairo-prismatic tilings which are not doubly periodic and therefore do not belong to a wallpaper group.

While it is still unknown whether the Cairo and prismatic tilings are perimeter-minimizing on the plane when we allow for mixtures of convex and nonconvex

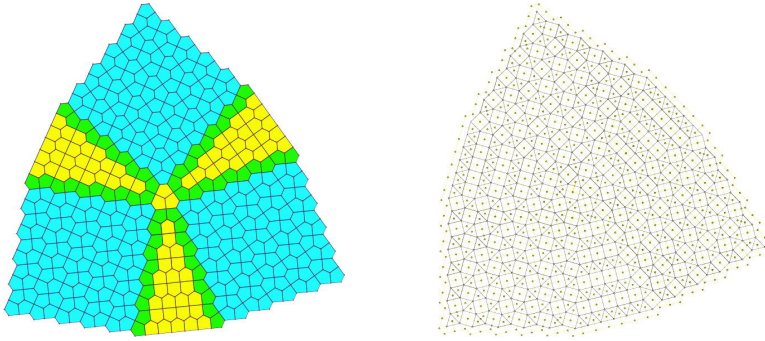


**Figure 18.** Windmill tiling (left) and its dual (right).

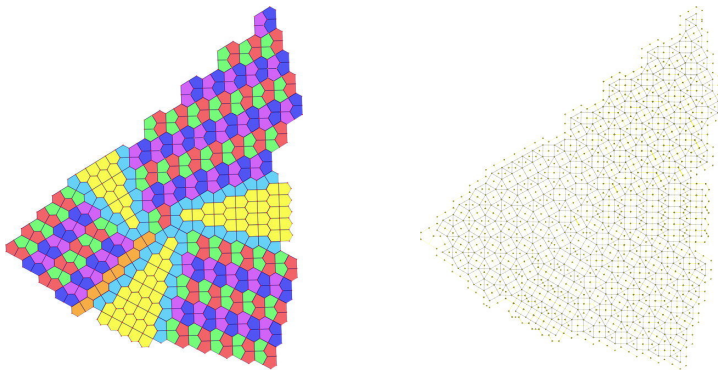


**Figure 19.** Chaos tiling (left) and its dual (right).

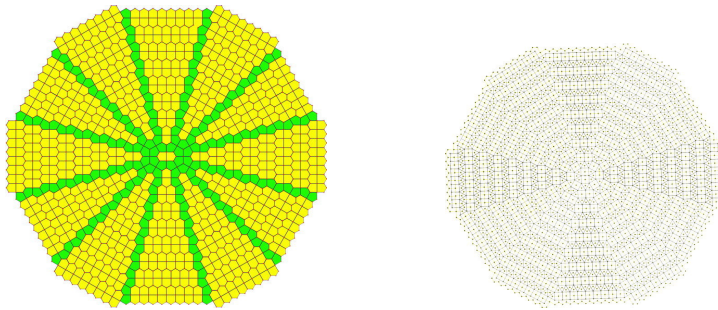


**Figure 20.** Plaza tiling (left) and its dual (right).

pentagons, we place bounds on the ratio of convex to nonconvex pentagons in order to rule out mixtures on certain flat tori.

**Proposition 2.10.** *A tiling by unit-area nonconvex pentagons has more perimeter per tile than a Cairo or prismatic pentagon.*

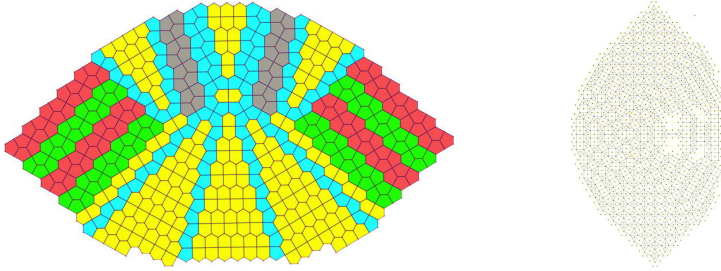


**Figure 21.** Bunny tiling (left) and its dual (right).

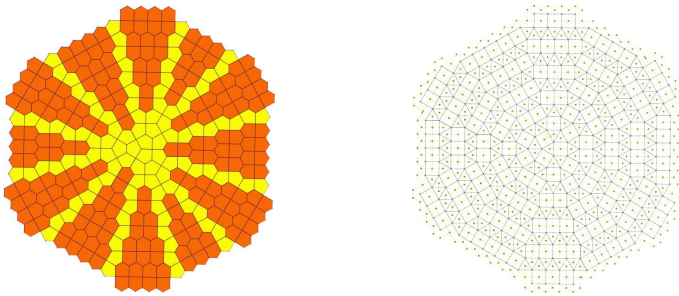


**Figure 22.** Tiling by Marjorie Rice from [Schattschneider 1981, Figure 15] (left) and its dual (right).

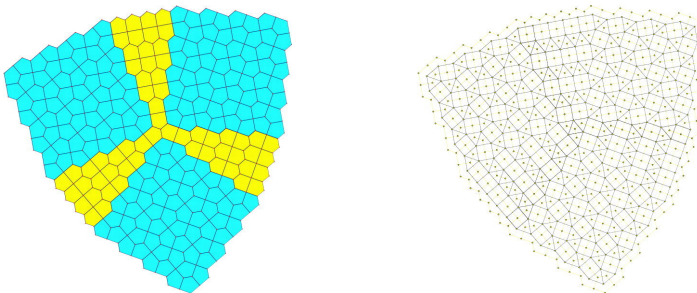


**Figure 23.** Waterwheel tiling (left) and its dual (right).

*Proof.* Indeed, we may show that any unit-area nonconvex pentagon has perimeter greater than 4. Any nonconvex pentagon has more perimeter than its convex hull, which is a quadrilateral or triangle and hence has at least the perimeter of a square or equilateral triangle.  $\square$

**Proposition 2.11.** *In a perimeter-minimizing tiling by unit-area pentagons, the ratio of convex to nonconvex pentagons must be greater than 2.6.*

*Proof.* The perimeters of a regular pentagon, Cairo and prismatic pentagons, and the unit square are  $P_0 = 2\sqrt{5}\sqrt[4]{5} - 2\sqrt{5} > 3.81$ ,  $P_1 = 2\sqrt{2 + \sqrt{3}} > 3.86$ , and 4.

Since all nonconvex pentagons must have perimeter greater than or equal to that of the unit square, we consider the limit case in which the perimeter of the nonconvex pentagons is  $P_2 = 4$ . The convex pentagons have perimeter greater than or equal to that of the regular pentagon,  $P_0$ . Note that

$$\frac{P_2 - P_1}{P_1 - P_0} > 2.6,$$

and thus the ratio of regular pentagons to squares must be greater than 2.6. It follows that the ratio of convex to nonconvex pentagons must be greater than 2.6.  $\square$

**Lemma 2.12.** *For a flat torus of area 2, a tiling by nonconvex and convex unit-area pentagons has perimeter greater than 3.9.*

*Proof.* The perimeter of any nonconvex unit-area pentagon must be greater than or equal to the perimeter of the unit square, and the perimeter of any convex unit-area pentagon must be greater than or equal to that of the regular pentagon,  $2\sqrt{5}\sqrt[4]{5} - 2\sqrt{5} > 3.8$ . Thus, the total perimeter of a tiling by both nonconvex and convex pentagons on the appropriate torus of area 2 must be greater than

$$\frac{3.8 + 4}{2} = 3.9. \quad \square$$

### 3. Minimal tilings on flat tori

This section identifies unique optimal tilings for some small flat tori. Our main result, Proposition 3.9, states that the unique perimeter-minimizing unit-area pentagonal tiling of the square torus of area 4 is by Cairo pentagons as shown in Figure 2. Similarly, Conjecture 3.4 states that the minimal pentagonal tiling of the square torus of area 2 is by squares as in Figure 27. Proposition 3.3 states that the unique perimeter-minimizing unit-area pentagonal tiling of a certain flat torus of area 2 is by prismatic pentagons (Figure 26).

Similarly, we investigate minimal polygonal tilings of other small flat tori and Klein bottles (Figure 35). Wedd [2009] proposes that a regular hexagonal torus of area  $A \in \mathbb{N}$  can be tiled by regular hexagons if and only if  $A = x^2 + xy + y^2$  where  $x, y \in \mathbb{N}$ ,  $A \neq 0$  (Proposition 3.10). By [Hales 2001, Theorem 3], it would follow that these are unique perimeter-minimizing tilings (Proposition 3.11). Many flat tori cannot be tiled by regular hexagons. We investigate the square tori of areas 2, 3, 4 and conjecture that the minimal tilings are as shown in Figures 33 and 34.

In these proofs, we do not assume that the tiles are convex. Hales [2001, Theorem 1] proved that one cannot improve on the regular hexagonal tiling by mixing in nonconvex tiles. Similarly, Chung et al. [2012, Section 1] conjectured that one cannot improve on Cairo-prismatic tilings by mixing in nonconvex pentagons. We prove such results for some small flat tori.

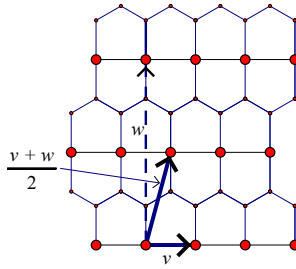


**Figure 24.** Lattice of prismatic tiling.

Proposition 3.1 characterizes flat tori that can be tiled by prismatic pentagons:

**Proposition 3.1.** *A flat torus can be tiled by prismatic pentagons if and only if its fundamental polygon is determined by integer linear combinations of*

$$\langle(\sqrt{6} - \sqrt{2}), 0\rangle \quad \text{and} \quad \langle(\sqrt{6} - \sqrt{2})/2, (\sqrt{6} + \sqrt{2})/2\rangle.$$

*Proof.* The prismatic tiling is the unique way to tile the plane with prismatic pentagons [Chung et al. 2012, Proposition 2.2]. The lattice of the tiling is generated by the two vectors  $\langle\sqrt{6} - \sqrt{2}, 0\rangle$  and  $\langle(\sqrt{6} - \sqrt{2})/2, (\sqrt{6} + \sqrt{2})/2\rangle$ , as shown in Figure 24. Therefore flat tori that can be tiled only by prismatic pentagons must have fundamental region determined by integer linear combinations of  $\langle\sqrt{6} - \sqrt{2}, 0\rangle$  and  $\langle(\sqrt{6} - \sqrt{2})/2, (\sqrt{6} + \sqrt{2})/2\rangle$ .

On the other hand, given a flat torus with fundamental polygon determined by integer linear combinations of  $\langle(\sqrt{6} - \sqrt{2}), 0\rangle$  and  $\langle(\sqrt{6} - \sqrt{2})/2, (\sqrt{6} + \sqrt{2})/2\rangle$ , one can cut it into many congruent parallelograms determined by vectors  $\langle(\sqrt{6} - \sqrt{2}), 0\rangle$  and  $\langle(\sqrt{6} - \sqrt{2})/2, (\sqrt{6} + \sqrt{2})/2\rangle$ , as shown in Figure 25. Each small parallelogram can be tiled by two prismatic pentagons. Thus the whole fundamental polygon can be tiled by prismatic pentagons as well.  $\square$

**Corollary 3.2.** *Prismatic pentagons do not tile a square torus.*

*Proof.* Suppose there exists a square torus that can be tiled by prismatic pentagons.

Let  $\mathbf{v} = \langle\sqrt{6} - \sqrt{2}, 0\rangle$  and  $\mathbf{w} = \langle 0, \sqrt{6} + \sqrt{2}\rangle$  (Figure 24). By Proposition 3.1, a torus tiled by prismatic pentagons has fundamental polygon determined by integer linear combinations of  $\mathbf{v}$  and  $(\mathbf{v} + \mathbf{w})/2$ . Let  $a\mathbf{v} + b\mathbf{w}$  and  $c\mathbf{v} + d\mathbf{w}$  be the two linearly independent vectors determining the fundamental polygon, where  $a$  and  $b$  are either both integers or both half-integers, and similarly for  $c$  and  $d$ .

Therefore

$$(a\mathbf{v} + b\mathbf{w}) \cdot (c\mathbf{v} + d\mathbf{w}) = 0 \quad \text{and} \quad |a\mathbf{v} + b\mathbf{w}| = |c\mathbf{v} + d\mathbf{w}|$$

which implies

$$ac|\mathbf{v}|^2 + bd|\mathbf{w}|^2 = 0$$

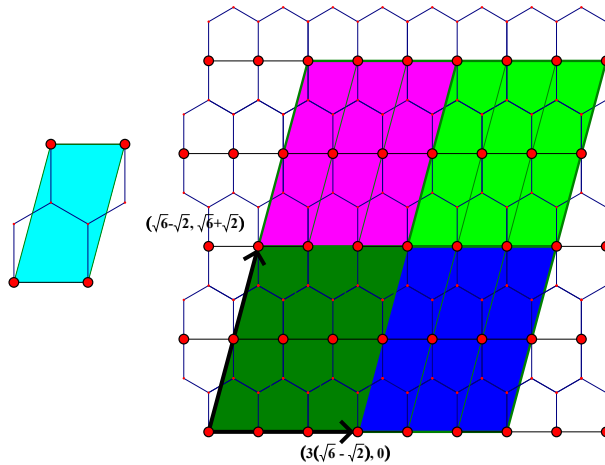


**Figure 25.** The unique perimeter-minimizing pentagonal tiling of a certain flat torus (Proposition 3.1).

since  $\mathbf{v}$  and  $\mathbf{w}$  are orthogonal to each other. Since  $|\mathbf{v}|^2 = 8 - 4\sqrt{3}$  is not a rational multiple of  $|\mathbf{w}|^2 = 8 + 4\sqrt{3}$ ,  $ac = bd = 0$ . Since  $a\mathbf{v} + b\mathbf{w}$  and  $c\mathbf{v} + d\mathbf{w}$  are nonzero, either  $a = d = 0$  or  $b = c = 0$ . Without loss of generality assume that  $b = c = 0$ .

As a result,  $(\sqrt{6} - \sqrt{2})a = |a\mathbf{v}| = |d\mathbf{w}| = (\sqrt{6} + \sqrt{2})d$ . Since  $(\sqrt{6} - \sqrt{2})$  is not a rational multiple of  $(\sqrt{6} + \sqrt{2})$ , at least one of  $a$  and  $d$  is irrational, which contradicts their definitions. Therefore no square torus can be tiled by prismatic pentagons.  $\square$

Proposition 3.3 provides an example of a special hexagonal torus utilizing only prismatic pentagons.

**Proposition 3.3.** *For a flat torus of area 2 defined by the two vectors  $\langle 2 - \sqrt{3}, 1 \rangle$  and  $\langle 2, 0 \rangle$ , the prismatic tiling is the unique perimeter-minimizing edge-to-edge pentagonal tiling as shown in Figure 26.*

*Proof.* Note that it is possible to tile this torus with only prismatic tiles (Figure 26), and this tiling has total perimeter  $2\sqrt{2} + \sqrt{3} < 3.87$ . Since a tiling by nonconvex and convex unit-area pentagons has perimeter greater than 3.9 on a flat torus of area 2 by Lemma 2.12, a perimeter-minimizing tiling is by two convex pentagonal tiles. Since this tiling must be doubly periodic, by [Chung et al. 2012, remark after Theorem 3.5] perimeter-minimizing tilings by convex pentagons are uniquely given by Cairo and prismatic tiles.

If there is at least one prismatic tile in the tiling, note that the base of this tile, which has length  $\sqrt{6} - \sqrt{2}$ , is unique among all the edges of the Cairo and prismatic pentagons. Since the tiling is edge-to-edge, the prismatic pentagon is consecutive to another prismatic pentagon rotated  $180^\circ$ . Thus these two pentagons tile the torus of area 2.



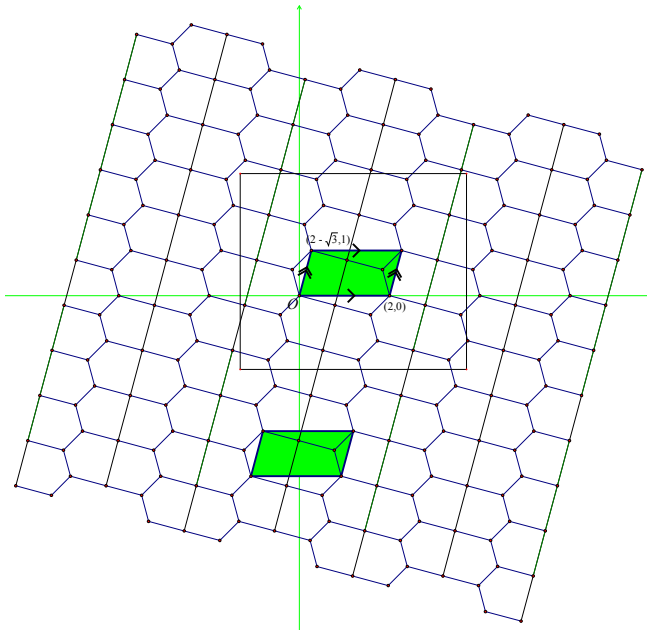


**Figure 26.** Prismatic Tiling on a flat torus of area 2 defined by the two vectors  $\langle 2 - \sqrt{3}, 1 \rangle$  and  $\langle 2, 0 \rangle$ .

If there is no prismatic tile, then the tiling consists of two Cairo pentagons. Since the short edge of the Cairo pentagon is unique, each Cairo pentagon is connected to another Cairo pentagon rotated  $180^\circ$ . Each of the two  $120^\circ$  angles between these two Cairo pentagons with two long adjacent edges can only fit in a third Cairo pentagon rotated  $90^\circ$ . Thus we have at least three pentagons that are not translational images of each other. Therefore they cannot all tile a flat torus of area 2.  $\square$

**Conjecture 3.4.** For a square torus of area 2, the unit-area square tiling is the unique perimeter-minimizing pentagonal tiling (Figure 27).

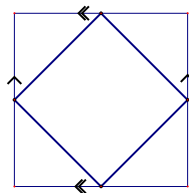


**Figure 27.** Conjectured perimeter-minimizing pentagonal tiling for the square torus of area 2.

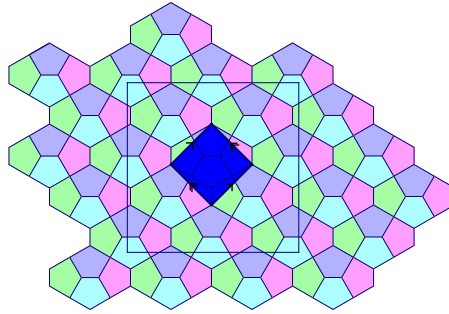


**Figure 28.** Cairo tiling on square torus of area 4.

We now prove that for the square torus of area 4, the perimeter-minimizing tiling is given by Cairo tiles as in Figure 28. In the process we prove some bounds on the perimeters of certain classes of pentagons.

**Lemma 3.5.** *A unit-area convex pentagon with one of the angles  $\alpha \in (0, \pi)$  has perimeter greater than or equal to*

$$P(\alpha) = 2 \sqrt{\tan \frac{\pi - \alpha}{2} + 4 \tan \frac{\pi + \alpha}{8}}.$$

*Proof.* By [Chung et al. 2012, Proposition 3.1], the uniquely perimeter-minimizing pentagon with angles  $a_i, i = 1, 2, \dots, 5$ , has perimeter

$$2 \sqrt{\sum_{i=1}^5 \cot \frac{a_i}{2}}.$$

Since the function  $\cot$  is strictly convex up to  $\pi/2$ , fixing an angle  $a_1 = \alpha$  and taking the other angles to be equal will give the minimal perimeter. Thus the minimum perimeter is

$$2 \sqrt{\cot \frac{\alpha}{2} + 4 \cot \frac{3\pi - \alpha}{8}} = 2 \sqrt{\tan \frac{\pi - \alpha}{2} + 4 \tan \frac{\pi + \alpha}{8}}. \quad \square$$

**Lemma 3.6.** *A unit-area pentagon with one of the edges  $s$  has perimeter greater than or equal to*

$$\frac{2\sqrt{2}(4 \sin(\theta/2) + \sin 2\theta)}{\sqrt{4 \sin \theta - \sin 4\theta}},$$

where  $\theta \in (0, \pi/2)$  is the only root of the equation

$$\frac{2\sqrt{2} \sin 2\theta}{\sqrt{4 \sin \theta - \sin 4\theta}} = s.$$

In fact,  $s$  is a strictly decreasing function of  $\theta$ .

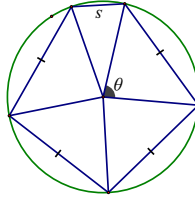


**Figure 29.** Perimeter-minimizing unit-area pentagon given an edge length.

*Proof.* First of all it is well known that, given the edge lengths  $s_i, i = 1, 2, \dots, 5$ , of a pentagon, the one inscribed in a circle has the maximum area. The area is

$$\frac{1}{2}r^2 \sum_{i=1}^5 \sin \theta_i,$$

where  $\theta_i$  is the angle at center corresponding to the edge  $s_i$ .

Since  $\sin$  is strictly concave down in the range  $[0, \pi]$ , the more nearly equal the angles, the larger the area given a fixed perimeter. Therefore, fixing one edge, the unit-area pentagon inscribed in a circle with the four other edges of equal length has the minimum perimeter.

Let  $r$  be the radius of the circumcircle and  $\theta \in (0, \pi/2)$  be the angle at center which corresponds to one of the 4 edges of same length (Figure 29).

Then the perimeter is

$$P = 2r \left( 4 \sin \frac{\theta}{2} + \sin \frac{2\pi - 4\theta}{2} \right) = 2r \left( 4 \sin \frac{\theta}{2} + \sin 2\theta \right),$$

and the area is

$$A = \frac{1}{2}r^2 (4 \sin \theta + \sin(2\pi - 4\theta)) = \frac{1}{2}r^2 (4 \sin \theta - \sin 4\theta) = 1,$$

since the pentagon has unit area. After substitution of  $r$ , we get

$$P = \frac{2\sqrt{2}(4 \sin(\theta/2) + \sin 2\theta)}{\sqrt{4 \sin \theta - \sin 4\theta}}.$$

On the other hand,

$$s = 2r \sin \frac{2\pi - 4\theta}{2} = 2r \sin 2\theta = \frac{2\sqrt{2} \sin 2\theta}{\sqrt{4 \sin \theta - \sin 4\theta}}.$$

Hence

$$\frac{ds}{d\theta} = - \frac{16\sqrt{2}(7 \cos(\theta/2) + 3 \cos(3\theta/2)) \sin^3(\theta/2)}{(4 \sin \theta - \sin 4\theta)^{3/2}} < 0,$$

for  $0 < \theta < \pi/2$ . Therefore  $s$  strictly decreases as  $\theta$  increases in the range  $(0, \pi/2)$ ; thus there is only one value of  $\theta$  for a given  $s$ . □

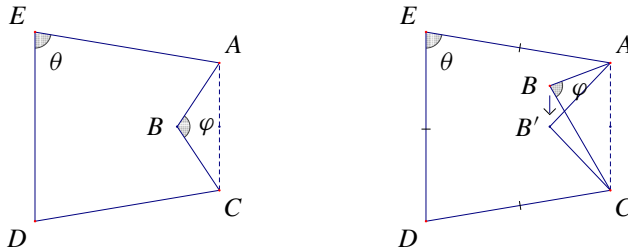


**Figure 30.** Left: perimeter-minimizing pentagon in Lemma 3.7. Right: translation of  $B$  to  $B'$  to reduce perimeter without affecting the area.

**Lemma 3.7.** A nonconvex unit-area pentagon  $ABCDE$  (Figure 30, left) satisfying

$$CD = DE = EA, \quad AB = BC, \quad \text{and} \quad DE \parallel AC$$

has perimeter

$$P(\theta, \varphi) = \sqrt{\frac{(3 + (1 - 2 \cos \theta) / \sin(\varphi/2))^2}{(1 - \cos \theta) \sin \theta - (0.5 - \cos \theta)^2 \cot(\varphi/2)'}}$$

where  $\varphi = \angle ABC < \pi$  and  $\theta = \angle AED = \angle CDE$ ,  $\pi/3 < \theta < \pi$ . In particular, for a fixed value of  $\theta$ ,  $P$  is a decreasing function of  $\varphi$ .

*Proof.* The formula for  $P(\theta, \varphi)$  can be determined by direct calculation. Notice that, if we fix all the vertices except  $B$ , and increase the value of  $\varphi$  up to  $\pi$ , we will get less perimeter but more area. Thus we can scale the pentagon to get unit area with less perimeter. Therefore the perimeter  $P$  is a decreasing function of  $\varphi$ .  $\square$

**Lemma 3.8.** Given positive real constants  $p, q, \varphi_0$  with  $p < q$  and  $\pi/2 < \varphi_0 \leq \pi$ , a unit-area nonconvex pentagon with an angle  $\phi = 2\pi - \varphi$  and two edges  $a, b$  adjacent to this angle that satisfies

$$p \leq a \leq b \leq q, \quad \frac{\pi}{2} \leq \varphi \leq \varphi_0,$$

has perimeter not less than

$$\inf_{\pi/3 < \theta < \pi} P(\theta, \varphi'(p, q, \varphi_0)),$$

where

$$\varphi'(a, b, \varphi) = 2 \tan^{-1} \left( \frac{a^2 + b^2 - 2ab \cos \varphi}{2ab \sin \varphi} \right).$$

*Proof.* For a nonconvex pentagon  $ABCDE$  with  $\angle ABC = \varphi \leq \pi$ ,  $|\overrightarrow{AB}| = a$ ,  $|\overrightarrow{BC}| = b$ , consider a line  $\ell$  parallel to  $\overrightarrow{AC}$  and a point  $B'$  on  $\ell$  that satisfies

$|\overrightarrow{AB'}| = |\overrightarrow{B'C}|$ .  $AB'CDE$  is also unit-area, but with less perimeter than  $ABCDE$  unless  $B = B'$  (Figure 30, right).

Let  $\angle AB'C = \varphi' \leq \pi$ ,  $c = |\overrightarrow{AC}|$  and  $h$  be the distance from  $B$  to  $AC$ . Then

$$c^2 = a^2 + b^2 - 2ab \cos \varphi, \quad ch = ab \sin \varphi, \quad c = 2h \tan \frac{\varphi'}{2}.$$

After simplification,

$$\tan \frac{\varphi'}{2} = \frac{a^2 + b^2 - 2ab \cos \varphi}{2ab \sin \varphi}.$$

Hence,

$$\begin{aligned} \frac{\partial}{\partial a} \tan \frac{\varphi'}{2} &= \frac{1}{2b \sin \varphi} \left( 1 - \frac{b^2}{a^2} \right) \leq 0, \\ \frac{\partial}{\partial b} \tan \frac{\varphi'}{2} &= \frac{1}{2a \sin \varphi} \left( 1 - \frac{a^2}{b^2} \right) \geq 0, \\ \frac{\partial}{\partial \varphi} \tan \frac{\varphi'}{2} &= \csc^2 \varphi \left( 1 - \frac{a^2 + b^2}{2ab} \cos \varphi \right) > 0, \end{aligned}$$

since  $a \leq b$  and  $\varphi \geq \pi/2$ . Therefore the maximum of  $\tan(\varphi'/2)$  is attained at the point where  $(a, b, \varphi) = (p, q, \varphi_0)$ . Since  $\tan$  is an increasing function in the range  $(0, \pi/2)$ , the maximum of  $\varphi'$  is attained at the same point; i.e.,

$$\varphi'(a, b, \varphi) \leq \varphi'(p, q, \varphi_0),$$

for all  $p \leq a \leq b \leq q$  and  $\pi/2 \leq \varphi \leq \varphi_0$ .

By Lemma 3.7, the perimeter of  $AB'CDE$  is a decreasing function of  $\angle AB'C$ ; therefore

$$\begin{aligned} \text{perim}(ABCDE) &\geq \text{perim}(AB'CDE) \\ &= P(\angle AED, \varphi'(a, b, \varphi)) \\ &\geq P(\angle AED, \varphi'(p, q, \varphi_0)) \\ &\geq \inf_{\pi/3 < \theta < \pi} P(\theta, \varphi'(p, q, \varphi_0)). \quad \square \end{aligned}$$

**Proposition 3.9.** *For a square torus of area 4, the Cairo tiling is the unique perimeter-minimizing edge-to-edge pentagonal tiling.*

*Proof.* Recall that the lower bounds on the perimeters of a convex and nonconvex unit-area pentagon are

$$P_{\text{convex}} \geq 2\sqrt{5} \sqrt[4]{5 - 2\sqrt{5}} > 3.81193, \quad P_{\text{nonconvex}} > 4,$$

since the perimeter-minimizing convex pentagon is a regular pentagon and the perimeter-minimizing nonconvex pentagon has more perimeter than a square. The

perimeter of each Cairo pentagon is  $2\sqrt{2 + \sqrt{3}} < 3.86371$ ; thus the total perimeter of the Cairo tiling on a square torus of area 4 is

$$P_C = \frac{1}{2} \times 4(2\sqrt{2 + \sqrt{3}}) < 7.72742.$$

Therefore the perimeter-minimizing tiling has total perimeter less than 7.72742.

If there are at least two nonconvex pentagons in a pentagonal tiling, the total perimeter will be greater than  $(3.81193 \times 2 + 4 \times 2)/2 = 7.81193 > 7.72742$ ; thus it is not perimeter-minimizing. Therefore a perimeter-minimizing tiling has at most one nonconvex pentagonal tile.

**Case 1: There is no nonconvex pentagonal tile.** Note that it is possible to tile this torus with only Cairo tiles (Figure 28). Since this tiling must be doubly periodic, by [Chung et al. 2012, remark after Theorem 3.5] perimeter-minimizing tilings by convex pentagons are uniquely given by Cairo and prismatic tiles.

*Case 1.1: The tiling consists of only Cairo pentagons.* This corresponds to a doubly periodic planar tiling by Cairo pentagons. By [Chung et al. 2012, Proposition 2.2] the Cairo tiling is the unique pentagonal planar tiling by Cairo tiles. Thus Figure 28 shows the unique perimeter-minimizing tiling in this case.

*Case 1.2: The tiling consists of only prismatic pentagons.* By Corollary 3.2, a square torus cannot be tiled by prismatic pentagons.

*Case 1.3: The tiling consists of both Cairo and prismatic pentagons.* Note that the length of the base of the prismatic pentagon is unique among all the edges of the Cairo and prismatic pentagons. Since the tiling is edge-to-edge, the prismatic pentagon is consecutive to another prismatic pentagon rotated  $180^\circ$ . The rest of the proof is presented with reference to Figure 31.

The pentagons are labeled with the same number if and only if they are trans-

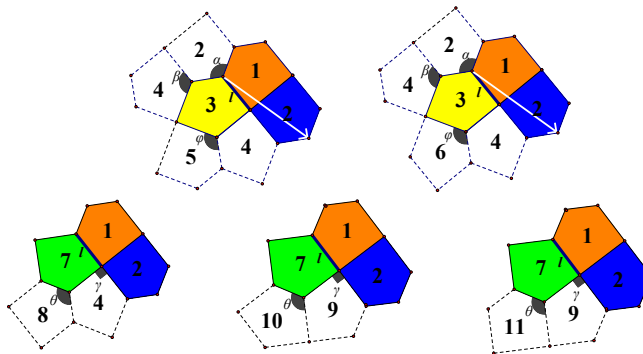


**Figure 31.** Proof of Case 1.3: A square torus of area 4 cannot be tiled by a mixture of Cairo and prismatic pentagons.

lational images. Label the two prismatic pentagons as 1 and 2. Consider the edge  $l$  of pentagon 1. There are only two ways to put a Cairo pentagon next to edge  $l$ , namely pentagon 3 or 7, so that the degrees of the two ends of  $l$  match up.

If pentagon 3 is used, note that there is only one way to put a Cairo or prismatic pentagon at angle  $\alpha$ , which is to put another prismatic pentagon 2. The only way to put a Cairo or prismatic pentagon at angle  $\beta$  is to put a Cairo pentagon 4.

Now we have four unit-area tiles that are not translational images of each other; therefore they are all the tiles of the square torus of area 4. As a result, the vector (white arrow) that brings one of the pentagons labeled 2 to the other is indeed a translation vector of the tiling. Thus pentagon 4 is also brought right next to the other pentagon 2. At angle  $\varphi$ , there are two ways to put a Cairo or prismatic pentagon, namely pentagon 5 or 6. On the other hand, neither of them is a translational image of pentagon 1, 2, 3 or 4; thus this cannot be a tiling of a square torus of area 4. If pentagon 7 is used, consider angle  $\gamma$ . There are two ways to put a Cairo or prismatic pentagon, namely pentagon 4 or 9. If pentagon 4 is used, there is only one way to put a Cairo or prismatic pentagon at angle  $\theta$ : pentagon 8. In this case we have five tiles, no two of which are translational images of each other; thus they cannot tile the square torus of area 4. Thus pentagon 9 has to be put at angle  $\gamma$ . There are two ways to put a Cairo or prismatic pentagon at angle  $\theta$ , namely pentagon 10 or 11. However, neither of them is a translational image of any of the other four pentagons. Thus, again, this cannot tile the square torus of area 4.

Therefore we can conclude that we cannot tile the square torus of area 4 with both Cairo and prismatic pentagons.

**Case 2: There is one nonconvex pentagonal tile.** Since the area of the torus is 4, there are three convex pentagonal tiles.

If there is a convex tile with perimeter greater than or equal to 3.831, the total perimeter will be greater than  $(3.81193 \times 2 + 3.831 + 4)/2 = 7.72743 > 7.72742$ , thus not perimeter-minimizing. Therefore the perimeter of each convex tile satisfies

$$3.81193 < P_{\text{convex}} < 3.831.$$

If the nonconvex tile has perimeter greater than or equal to 4.0191, the total perimeter will be greater than  $(3.81193 \times 3 + 4.0191)/2 = 7.727445 > 7.72742$ , thus not perimeter-minimizing. Therefore the perimeter of the nonconvex tile satisfies

$$4 < P_{\text{nonconvex}} < 4.0191.$$

Consider the interior angles of the convex tiles. Note that for  $\alpha \geq 1.5792$  or  $\alpha \leq 2.2341$ , a convex pentagon with an angle  $\alpha$  has perimeter greater than or equal to  $P(\alpha) > 3.831$  by Lemma 3.5. Thus the convex tiles in a perimeter-minimizing tiling have interior angles within the range  $(1.5792, 2.2341)$ .

Now consider the edge lengths of the convex tiles. By Lemma 3.6 and the fact that  $3.81193 < P < 3.831$ ,

$$\frac{2\sqrt{2}(4 \sin(\theta/2) + \sin 2\theta)}{\sqrt{4 \sin \theta - \sin 4\theta}} < 3.831;$$

thus

$$1.1565 < \theta < 1.3564.$$

Since  $s$  is a decreasing function of  $\theta$ , we can get a bound on the edge length  $s$  of a convex tile:

$$0.5444 < s < 0.9659.$$

Consider the nonconvex pentagonal tile  $ABCDE$  with a reflex  $\angle ABC$ . Since the interior angles of the convex tiles are greater than  $1.5792 > \pi/2$ , if the point  $B$  has degree at least 3, the total angle at that point will be greater than  $\pi + (\pi/2) \times 2 = 2\pi$ , a contradiction. Therefore the nonconvex angle has degree 2. In this case  $\angle ABC$  is an interior angle of a convex tile; thus

$$1.5792 < \angle ABC < 2.2341 \quad \text{and} \quad 0.5444 < AB, BC < 0.9659.$$

By Lemma 3.8, the perimeter of  $ABCDE$  is not less than

$$\inf_{\pi/3 < \theta < \pi} P(\theta, \varphi'(0.5444, 0.9659, 2.2341)),$$

where

$$\varphi'(a, b, \varphi) = 2 \tan^{-1} \frac{a^2 + b^2 - 2ab \cos \varphi}{2ab \sin \varphi}$$

and

$$P(\theta, \varphi) = \sqrt{\frac{4(1.5 + (0.5 - \cos \theta)/\sin(\varphi/2))^2}{(1 - \cos \theta) \sin \theta - (0.5 - \cos \theta)^2 \cot(\varphi/2)}}.$$

After direct computation, the minimum is greater than  $4.078 > 4.0191$ . Therefore, in this case, the tiling will not be perimeter-minimizing. □

Some regular hexagonal tori can be tiled by regular hexagons. Wedd [2009] states without proof that for a regular hexagonal torus of area  $A$ , where  $A > 0$ , a tiling by regular hexagons exists if and only if  $A = x^2 + xy + y^2$  for some nonnegative integers  $x, y$ . We give a complete proof of Wedd's statement. By [Hales 2001, Theorem 3], this would be the unique perimeter-minimizing tiling of such a torus.

**Proposition 3.10** [Wedd 2009]. *A regular hexagonal torus with area  $A$ , where  $A \neq 0$ , can be tiled by regular hexagons with unit area if and only if  $A = x^2 + xy + y^2$ , where  $x, y$  are nonnegative integers.*



*Proof.* First we shall prove that a regular hexagonal torus with  $A = x^2 + xy + y^2$  can be tiled by regular hexagons. Our approach is to start with a unit-area hexagonal tiling of the plane, then find a regular hexagon with area  $A$  so that the tiling also tiles the torus formed by identifying opposite edges of this hexagon.

On a planar tiling by unit-area regular hexagons, construct the complex plane as follows: pick the center of one of the hexagons as the origin, and one of the vertices of the same hexagon as the point  $p$ , where  $p \in \mathbb{R}$  ( $p > 0$ ) is the distance between the vertex and the center. Let  $\zeta = e^{\pi i/3}$  be a primitive sixth root of unity. Consider the triangular lattice  $L$  formed by the vertices and centers of all the hexagons. It is generated by two points  $p$  and  $q$ , where  $q = p\zeta$ . Let  $x, y$  be nonnegative integers such that  $A = x^2 + xy + y^2$ . Note that

$$|xp + yq| = |x + y\zeta|p = p\sqrt{x^2 + y^2 + xy} = p\sqrt{A}.$$

Therefore the area of the regular hexagon with vertices

$$xp + yq, (xp + yq)\zeta, (xp + yq)\zeta^2, (xp + yq)\zeta^3, (xp + yq)\zeta^4, (xp + yq)\zeta^5$$

is  $A$  times the area of the hexagon with vertices  $p, p\zeta, p\zeta^2, p\zeta^3, p\zeta^4, p\zeta^5$ , which is precisely the unit-area hexagon centered at the origin. It is left to verify that the torus  $T$  formed by identifying opposite edges of the big hexagon is tiled by the unit-area hexagons.

Note that a tiling of a flat torus corresponds to a doubly periodic tiling of the plane, with translational vectors given by the vectors that define the fundamental parallelogram. In our case, the fundamental parallelogram of the torus  $T$  is spanned by  $(xp + yq) + (xp + yq)\zeta$  and  $(xp + yq)\zeta + (xp + yq)\zeta^2$ , as one may verify. These two vectors send a lattice point in  $L$  to another lattice point in  $L$ . Furthermore, in the lattice  $L$ , a point  $ap + bq$ , with  $a, b \in \mathbb{Z}$ , is the center of a hexagonal tile if and only if  $3 \mid a - b$ . Since

$$\begin{aligned} (xp + yq) + (xp + yq)\zeta &= (x - y)p + (2y + x)q, \\ (xp + yq)\zeta + (xp + yq)\zeta^2 &= (-x - 2y)p + (2x + y)q, \end{aligned}$$

and 3 divides both  $(2y + x) - (x - y)$  and  $(2x + y) - (-x - 2y)$ , both vectors send centers to centers and vertices to vertices. As a result, these two vectors send  $L$  to itself. Therefore we can conclude that the unit-area hexagonal tiling is a tiling of the torus  $T$ . This is the desired tiling of the regular hexagonal torus with area  $A = x^2 + xy + y^2$ .

The converse is true since the vertices of the big hexagon all lie on the lattice  $L$ . Scale the lattice  $L$  so that  $p = 1$ ; then the distance between any two lattice points is  $x^2 + y^2 + 2xy \cos(4\pi/3) = x^2 + xy + y^2$  for some nonnegative integers  $x$  and  $y$ .

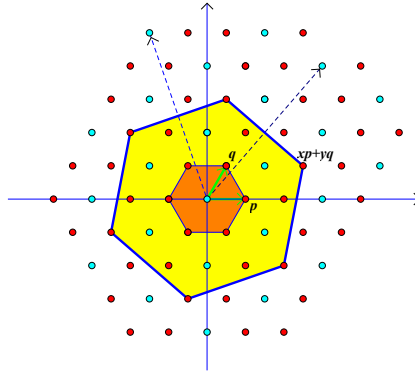


**Figure 32.** Illustration of the proof of Proposition 3.10 in the case when  $A = 7$ .

Thus the area of the original hexagon will be  $x^2 + xy + y^2$  times the area of each hexagonal tile, which is 1 in our case, as desired.  $\square$

**Proposition 3.11.** *A regular hexagonal tiling is the unique perimeter-minimizing unit-area tiling of any regular hexagonal torus of area  $A = x^2 + xy + y^2$ , where  $x, y$  are nonnegative integers.*

*Proof.* This is a direct result of [Hales 2001, Theorem 3] and Proposition 3.10.  $\square$

**Remark.** There exists no flat torus whose fundamental polygon is a pentagon with interior angles less than  $\pi$ .

To investigate polygonal tilings of quadrilateral tori we also present conjectures on the best way to tile a square torus. While the Cairo tiling is the best pentagonal tiling of the square torus of area 4, it may not be the perimeter-minimizing tiling of the square torus in general.

**Conjecture 3.12.** For the square tori of areas 2, 3, and 4, perimeter-minimizing unit-area tilings are given by the hexagonal tilings with dimensions as shown in Figures 33 and 34.

We conclude with some results on Klein bottles.

**Proposition 3.13.** *For a flat Klein bottle of integer area  $A$ , any unit-area tiling has perimeter greater than or equal to  $A/2$  times the perimeter of a unit-area regular hexagon. Equality is attained if and only if each tile is a regular hexagon.*

*Proof.* Since there exists a flat torus that double covers each flat Klein bottle, as shown in Figure 35, left, each tiling of a Klein bottle corresponds to a tiling of a certain flat torus. If there existed a tiling of a Klein bottle that had less perimeter than  $A/2$  times the perimeter of a unit-area regular hexagon, then there would exist a tiling of a flat torus that has a smaller perimeter ratio than the regular hexagonal

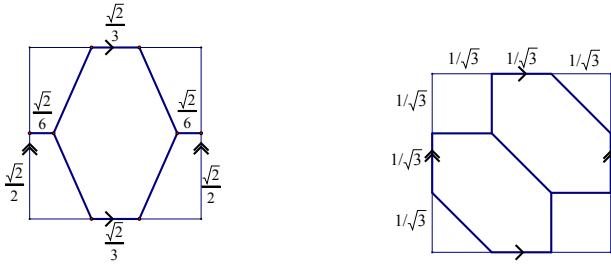


**Figure 33.** Proposed perimeter-minimizing tilings for the square torus of area 2 (left) and the square torus of area 3 (right).

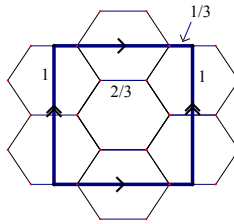


**Figure 34.** Proposed perimeter-minimizing tiling for the square torus of area 4.

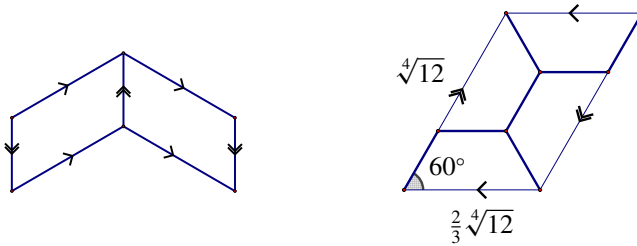


**Figure 35.** Left: every Klein bottle is double-covered by some flat torus. Right perimeter-minimizing tiling of a certain Klein bottle of area 2.

tiling. This would contradict the honeycomb conjecture [Hales 2001, Theorem 3]. □

**Example 3.14.** For the Klein bottle of area 2 of Figure 35, right, the unique perimeter-minimizing tiling is by regular hexagons.

**Acknowledgements**

We thank our advisor Frank Morgan for his patience and invaluable input. We also thank the 2010 SMALL Geometry Group, Zane Martin of the 2012 SMALL

Geometry Group, Doris Schattschneider, Marjorie Senechal, Daniel Huson, and Chaim Goodman-Strauss for their help.

For funding, we thank the National Science Foundation for grants to Professor Morgan and to the Williams College SMALL Research Experience for Undergraduates; Williams College for additional funding; and the Mathematical Association of America for supporting our trip to talk at the 2011 MathFest.

## References

- [Chung et al. 2012] P. N. Chung, M. A. Fernandez, Y. Li, M. Mara, F. Morgan, I. R. Plata, N. Shah, L. S. Vieira, and E. Wikner, “Isoperimetric pentagonal tilings”, *Notices Amer. Math. Soc.* **59**:5 (2012), 632–640. MR 2954290 Zbl 06092121
- [Hales 2001] T. C. Hales, “The honeycomb conjecture”, *Discrete Comput. Geom.* **25**:1 (2001), 1–22. MR 2002a:52020 Zbl 1007.52008
- [Huson and Westphal  $\geq$  2014] D. Huson and K. Westphal, “2DTiler”, interactive tiling program, Eberhard Karls Universität Tübingen, <http://goo.gl/pl9Wq>.
- [Li et al. 2011] Y. Li, M. Mara, I. R. Plata, and E. Wikner, “Optimal planar tilings with vertex penalties”, preprint, 2011.
- [Rice  $\geq$  2014] M. Rice, “Intriguing tessellations”, web article, <http://goo.gl/uKavk>.
- [Schattschneider 1978] D. Schattschneider, “The plane symmetry groups: their recognition and notation”, *Amer. Math. Monthly* **85**:6 (1978), 439–450. MR 57 #17476 Zbl 0381.20036
- [Schattschneider 1981] D. Schattschneider, “In praise of amateurs”, pp. 140–166 in *The Mathematical Gardner*, edited by D. Klamer, Prindle, Weber & Schmidt, Boston, 1981.
- [Wedd 2009] N. S. Wedd, “Regular maps in the torus, with hexagonal faces”, website, 2009, <http://www.weddslist.com/groups/genus/1/hex.php>.
- [Wikipedia Commons 2011] Wikipedia, “Wallpaper group”, website, 2011, [http://en.wikipedia.org/wiki/Wallpaper\\_group](http://en.wikipedia.org/wiki/Wallpaper_group).

Received: 2012-03-29 Accepted: 2012-05-26

briancpn@mit.edu	<i>Department of Mathematics, Massachusetts Institute of Technology, 305 Memorial Drive, Cambridge, MA 02139, United States</i>
maf2831@truman.edu	<i>Mathematics and Computer Science Department, Truman State University, 100 E. Normal Avenue, Kirksville, MO 63501, United States</i>
niraleekshah@gmail.com	<i>Department of Mathematics and Statistics, Bronfman Science Center, Williams College, Williamstown, MA 01267, United States</i>
dw8603@wayne.edu	<i>Department of Mathematics, Wayne State University, 656 W. Kirby, Detroit, MI 48202, United States</i>
elena.wikner@gmail.com	<i>Department of Mathematics and Statistics, Bronfman Science Center, Williams College, Williamstown, MA 01267, United States</i>

# involve

msp.org/involve

## EDITORS

### MANAGING EDITOR

Kenneth S. Berenhaut, Wake Forest University, USA, berenhks@wfu.edu

### BOARD OF EDITORS

Colin Adams	Williams College, USA colin.c.adams@williams.edu	David Larson	Texas A&M University, USA larson@math.tamu.edu
John V. Baxley	Wake Forest University, NC, USA baxley@wfu.edu	Suzanne Lenhart	University of Tennessee, USA lenhart@math.utk.edu
Arthur T. Benjamin	Harvey Mudd College, USA benjamin@hmc.edu	Chi-Kwong Li	College of William and Mary, USA ckli@math.wm.edu
Martin Bohner	Missouri U of Science and Technology, USA bohner@mst.edu	Robert B. Lund	Clemson University, USA lund@clemson.edu
Nigel Boston	University of Wisconsin, USA boston@math.wisc.edu	Gaven J. Martin	Massey University, New Zealand g.j.martin@massey.ac.nz
Amarjit S. Budhiraja	U of North Carolina, Chapel Hill, USA budhiraj@email.unc.edu	Mary Meyer	Colorado State University, USA meyer@stat.colostate.edu
Pietro Cerone	La Trobe University, Australia P.Cerone@latrobe.edu.au	Emil Minchev	Ruse, Bulgaria eminchev@hotmail.com
Scott Chapman	Sam Houston State University, USA scott.chapman@shsu.edu	Frank Morgan	Williams College, USA frank.morgan@williams.edu
Joshua N. Cooper	University of South Carolina, USA cooper@math.sc.edu	Mohammad Sal Moselehian	Ferdowsi University of Mashhad, Iran moslehian@ferdowsi.um.ac.ir
Jem N. Corcoran	University of Colorado, USA corcoran@colorado.edu	Zuhair Nashed	University of Central Florida, USA znashed@mail.ucf.edu
Toka Diagana	Howard University, USA tdiagana@howard.edu	Ken Ono	Emory University, USA ono@mathcs.emory.edu
Michael Dorff	Brigham Young University, USA mdorff@math.byu.edu	Timothy E. O'Brien	Loyola University Chicago, USA tobrie1@luc.edu
Sever S. Dragomir	Victoria University, Australia sever@matilda.vu.edu.au	Joseph O'Rourke	Smith College, USA orourke@cs.smith.edu
Behrouz Emamizadeh	The Petroleum Institute, UAE bemamizadeh@pi.ac.ae	Yuval Peres	Microsoft Research, USA peres@microsoft.com
Joel Foisy	SUNY Potsdam foisyjs@potsdam.edu	Y.-F. S. Pétermann	Université de Genève, Switzerland petermann@math.unige.ch
Errin W. Fulp	Wake Forest University, USA fulp@wfu.edu	Robert J. Plemmons	Wake Forest University, USA rplemmons@wfu.edu
Joseph Gallian	University of Minnesota Duluth, USA jgallian@d.umn.edu	Carl B. Pomerance	Dartmouth College, USA carl.pomerance@dartmouth.edu
Stephan R. Garcia	Pomona College, USA stephan.garcia@pomona.edu	Vadim Ponomarenko	San Diego State University, USA vadim@sciences.sdsu.edu
Anant Godbole	East Tennessee State University, USA godbole@etsu.edu	Bjorn Poonen	UC Berkeley, USA poonen@math.berkeley.edu
Ron Gould	Emory University, USA rg@mathcs.emory.edu	James Propp	U Mass Lowell, USA jpropp@cs.uml.edu
Andrew Granville	Université Montréal, Canada andrew@dms.umontreal.ca	József H. Przytycki	George Washington University, USA przytyck@gwu.edu
Jerrold Griggs	University of South Carolina, USA griggs@math.sc.edu	Richard Rebarber	University of Nebraska, USA rrebarbe@math.unl.edu
Sat Gupta	U of North Carolina, Greensboro, USA sngupta@uncg.edu	Robert W. Robinson	University of Georgia, USA rwr@cs.uga.edu
Jim Haglund	University of Pennsylvania, USA jhaglund@math.upenn.edu	Filip Saidak	U of North Carolina, Greensboro, USA f_saidak@uncg.edu
Johnny Henderson	Baylor University, USA johnny_henderson@baylor.edu	James A. Sellers	Penn State University, USA sellersj@math.psu.edu
Jim Hoste	Pitzer College jhoste@pitzer.edu	Andrew J. Sterge	Honorary Editor andy@ajsterge.com
Natalia Hritonenko	Prairie View A&M University, USA nahritonenko@pvamu.edu	Ann Trenk	Wellesley College, USA atrenk@wellesley.edu
Glenn H. Hurlbert	Arizona State University, USA hurlbert@asu.edu	Ravi Vakil	Stanford University, USA vakil@math.stanford.edu
Charles R. Johnson	College of William and Mary, USA crjohnso@math.wm.edu	Antonia Vecchio	Consiglio Nazionale delle Ricerche, Italy antonia.vecchio@cnr.it
K. B. Kulasekera	Clemson University, USA kk@ces.clemson.edu	Ram U. Verma	University of Toledo, USA verma99@msn.com
Gerry Ladas	University of Rhode Island, USA gladas@math.uri.edu	John C. Wierman	Johns Hopkins University, USA wierman@jhu.edu
		Michael E. Zieve	University of Michigan, USA zieve@umich.edu

## PRODUCTION

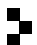
Silvio Levy, Scientific Editor

See inside back cover or msp.org/involve for submission instructions. The subscription price for 2014 is US \$120/year for the electronic version, and \$165/year (+\$35, if shipping outside the US) for print and electronic. Subscriptions, requests for back issues from the last three years and changes of subscribers address should be sent to MSP.

Involve (ISSN 1944-4184 electronic, 1944-4176 printed) at Mathematical Sciences Publishers, 798 Evans Hall #3840, c/o University of California, Berkeley, CA 94720-3840, is published continuously online. Periodical rate postage paid at Berkeley, CA 94704, and additional mailing offices.

Involve peer review and production are managed by EditFLOW<sup>®</sup> from Mathematical Sciences Publishers.

PUBLISHED BY

 **mathematical sciences publishers**  
nonprofit scientific publishing

<http://msp.org/>

© 2014 Mathematical Sciences Publishers

# involve

2014

vol. 7

no. 4

Whitehead graphs and separability in rank two	431
MATT CLAY, JOHN CONANT AND NIVETHA RAMASUBRAMANIAN	
Perimeter-minimizing pentagonal tilings	453
PING NGAI CHUNG, MIGUEL A. FERNANDEZ, NIRALEE SHAH, LUIS SORDO VIEIRA AND ELENA WIKNER	
Discrete time optimal control applied to pest control problems	479
WANDI DING, RAYMOND HENDON, BRANDON CATHEY, EVAN LANCASTER AND ROBERT GERMICK	
Distribution of genome rearrangement distance under double cut and join	491
JACKIE CHRISTY, JOSH MCHUGH, MANDA RIEHL AND NOAH WILLIAMS	
Mathematical modeling of integrin dynamics in initial formation of focal adhesions	509
AURORA BLUCHER, MICHELLE SALAS, NICHOLAS WILLIAMS AND HANNAH L. CALLENDER	
Investigating root multiplicities in the indefinite Kac–Moody algebra $E_{10}$	529
VICKY KLIMA, TIMOTHY SHATLEY, KYLE THOMAS AND ANDREW WILSON	
On a state model for the $SO(2n)$ Kauffman polynomial	547
CARMEN CAPRAU, DAVID HEYWOOD AND DIONNE IBARRA	
Invariant measures for hybrid stochastic systems	565
XAVIER GARCIA, JENNIFER KUNZE, THOMAS RUDELIUS, ANTHONY SANCHEZ, SIJING SHAO, EMILY SPERANZA AND CHAD VIDDEN	

